AUTOMATIC EXPERIMENTAL DESIGN USING DEEP GENERATIVE MODELS OF ORBITAL DATA

Alberto Candela[1], David R. Thompson[2], David Wettergreen[1]

[1]*Robotics Institute, Carnegie Mellon University, Pittsburgh, PA, USA*
E-mail: albertoc@cmu.edu, dsw@cmu.edu
[2]*Jet Propulsion Laboratory, California Institute of Technology, Pasadena, CA, USA*
E-mail: David.R.Thompson@jpl.nasa.gov

ABSTRACT

The mapping and characterization of planetary surfaces relies on the analysis of data collected by spacecraft and orbiters. Their instruments provide extensive contextual information, but factors such as sparsity, resolution, and noise leave uncertainty in the orbital analysis. Hence the need to send robotic explorers to refine these models through the collection of definitive, *in situ* measurements. Since planetary rovers face many operational challenges and constraints, it is important to identify sampling locations that maximize information value. This paper describes a deep generative method that learns a probabilistic model relating remote and *in situ* data, which then allows formal experimental design and measurement planning using tools from information theory. We apply this method to spectroscopic observations of the Cuprite Hills in Nevada. The results indicate that our model is capable of inferring high resolution features from orbital data, and that it also identifies effective *in situ* sampling locations.

1 INTRODUCTION

The study of planetary surfaces has been made possible through the analysis of data collected by spacecraft and orbiters. For example, the instruments carried by the Mars Reconnaissance Orbiter (MRO) have been crucial in the mapping of landforms, minerals, and ice of Mars [1]. Despite the fact that these instruments provide useful information, factors such as sparsity, resolution, and noise leave uncertainty in the analysis of relatively low-resolution (10s of meters) remote sensing from orbit. Figure 1 shows an example of this phenomenon using MRO's Compact Reconnaissance Imaging Spectrometer for Mars (CRISM) sensor [2]. Important spectra features are lost due to the smoothing effect of imaging over large areas. Noise from the detector and the observed environment are apparent. For more definitive results, robotic explorers, such as Curiosity and ExoMars, are needed to collect high resolution, *in situ* measurements. Nonetheless, rovers face many operational challenges and constraints, so it is important to identify locations that maximize information value.

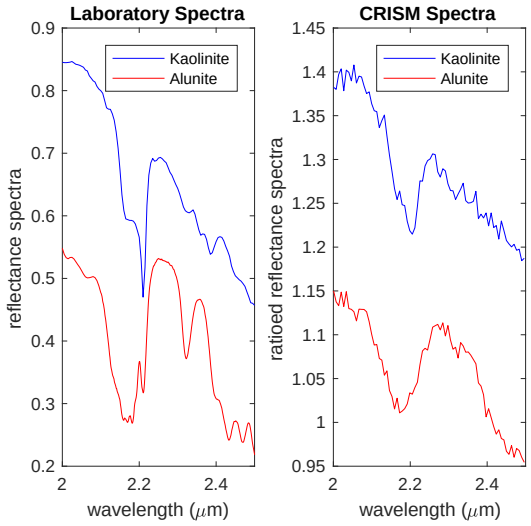

Figure 1: Comparison of high-quality laboratory spectra [3] (left) and CRISM ratioed spectra [4] (right), colored according to mineralogic match. The CRISM spectra from orbit shows feature smoothing due to resolution and noise from various sources.

Deep learning has enabled machines to automatically perform complex, nonlinear data modeling and analysis. In this work, we apply deep learning to inferring high resolution features from orbital data, and then help guide *in situ* explorers in their investigation in an efficient manner. Our approach integrates concepts from different networks and applications. Furthermore, our formulation is unsupervised, learning underlying patterns without the need for labeled data, which is difficult to obtain when studying distant planets.

Distribution-based models can be used to compute the associated uncertainty of the predictions using information-theoretic value functions [5]. Consequently, methods from autonomous science and

automatic experimental design may be applied to optimize scientific productivity when guiding rovers [6, 7, 8, 9, 10].

We apply these models and methods to imaging spectroscopy and the geologic analysis of spectra. We validate our deep learning model in a case study of the thoroughly-studied, mineralogically diverse site of Cuprite, Nevada [11]. Afterwards, we compute information-theoretic values to show the underlying uncertainty of each site, revealing informative sampling locations for an *in situ* explorer. Our results indicate that the deep generative model is a powerful tool for inferring high resolution features from low resolution orbital data.

2 FORMULATION

Our method of exploration is formulated as a process of model refinement (improving the accuracy, resolution and completeness of the surface model) and *in situ* sample selection to increase available information. Constituent techniques include generative models and experimental design.

Deep generative models learn probabilistic models of data in an unsupervised manner [12]. They have been successfully applied on many different scenarios, such as chemical design [13] and localization of celestial bodies [14]. The application that is of particular interest to this work is super-resolution, and it consists in the construction of high resolution models from low resolution input data [15]. Different deep generative models have led to impressive results in image generation and reconstruction [16, 17].

Within the family of deep generative models, two commonly-used methods are Generative Adversarial Networks (GAN) [18] and Variational Autoencoders (VAE) [19]. As the name indicates, a GAN is a system of two neural networks contesting with each other in order to learn how to best generate data. One network learns to generate candidates while the other learns to evaluate candidate fitness. GANs do not perform any transparent probability density estimation. Regarding VAEs, they learn a representation for a set of data by encoding into a latent or compressed space and then decoding back into the original state. VAEs make strong assumptions concerning the distribution of data, usually setting a multivariate Gaussian prior over the latent variables. In our particular case, VAEs are preferred because they can perform explicit density estimation; a property that can be used to advantage during information-driven exploration.

Learning explicit probability densities allows computation of the associated Shannon entropy, an information-theoretic value used to quantify the uncertainty of a prediction [5]. There exist extensive reviews of approaches for the problem of experimental design under probabilistic or Bayesian scenarios [20]. Under some weak assumptions that apply to most practical cases, it has been shown that one can employ a strategy known as maximum entropy sampling [21], which reflects the idea that in order to learn the most about a system under study, one should make observations where prior information is most uncertain. In other words, sampling well-known locations will only result in marginal benefits.

The aforementioned notions have been extensively applied on autonomous robotic exploration focusing on science survey tasks. They have been used for meteorite identification in Antarctica [6] and for selective data return in the Atacama Desert in Chile [7]. Recent efforts have incorporated more sophisticated path planning methods into the Bayesian experimental design problem with autonomous rovers [8, 9, 10].

3 METHOD

This work addresses the problem of identifying appropriate sampling locations for an explorer when the underlying task is to efficiently map and characterize a locally unknown area, such as a planetary surface. Specifically, a preliminary assessment where there is only access to non-labeled low-resolution observation of the scene.

We assume that a relationship between *in situ* data X and remote-sensed data Y exists, meaning $f : X \mapsto Y$. We define this process in a broad sense (it may be linear or nonlinear), but assume that it includes two characteristics. Orbital data tend to have a *lower resolution* than *in situ* data, and usually contain additional *noise*.

To solve the aforementioned problem, we propose the following strategy. First, use a *deep generative model* that learns a probabilistic model that predicts high-resolution data from low-resolution observations. Then, utilize *maximum entropy sampling* to identify the most informative sampling locations, given the learned probabilistic model.

3.1 Deep Generative Model

We use the basic structure of a VAE for learning Gaussian representations of data $\mathcal{N}_n(\mu, \Sigma)$ in

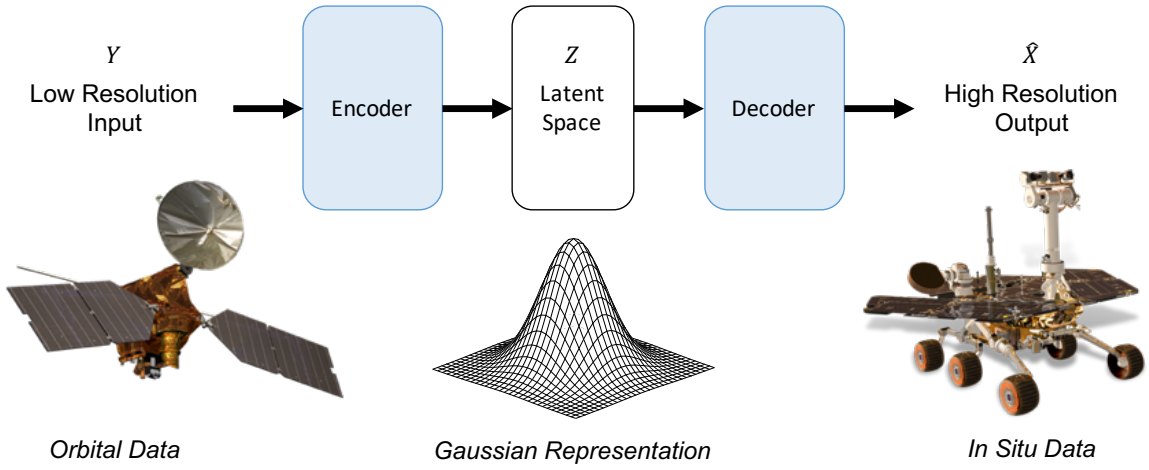

Figure 2: Basic structure of our deep generative model. The low resolution input is associated with an orbital measurement Y which is encoded into a multivariate Gaussian distribution $\mathcal{N}_n(\mu, \Sigma)$ in a latent space Z. This probabilistic representation is decoded into a high resolution output that is much richer in terms of information and feature content, and would correspond to the prediction of an in situ observation $\hat{X}$.

a latent or compressed space Z. By definition, a VAE is an autoencoder, so the input and the output should have the same resolution. However, we modify the previous notion in order to be able to incorporate different types of inputs and outputs; orbital and *in situ*, respectively (Figure 2).

Our model uses the following loss function:

$$L = E(\hat{X}, X) + \lambda D_{KL}\left(\mathcal{N}_n(\mu, \Sigma) || \mathcal{N}_n(0, 1)\right). \quad (1)$$

It adds two different types of loss terms: the reconstruction error between the predicted and the true output, and a Kullback-Leibler divergence penalization of the latent space with respect to a standard Gaussian. This results in a trade-off between reconstruction accuracy and learning meaningfulness, which is tuned by parameter λ.

We have presented this approach in a very general way. The specific details of an architecture depend enormously on its particular application and associated type of processed data. In this paper, we apply this model to imaging spectroscopy and the geologic analysis of spectra. We next explain the corresponding architecture details.

3.1.1 Deep Learning Architecture

Given the characteristics of spectral analysis, the scale or norm of a reflectance spectrum signal is irrelevant for material identification [22]. Hence, we perform a preprocessing step on the data that consists in L_∞ or max-normalization.

The relevant elements for the architecture of the deep generative model are the following: the encoder, latent space, decoder consist of one fully-connected layer each, with a ReLU activation function. The output layer also contains one fully-connected layer, but instead uses a sigmoid activation function. The dimensionality of the latent space is 5. The reconstruction loss consists in a mean squared error (MSE) criterion. The KL divergence coefficient λ is set to 5×10^{-5}. The optimization algorithm is Adam [23] with a mini-batch size of 32, and 50 training epochs.

3.2 Automatic Experimental Design

Once density estimation has been performed, Shannon entropy can be computed in order to quantify the associated uncertainty of the predictions [5]. It is defined as:

$$H(Z) = -\sum_{z \in Z} p(z) \log p(z). \quad (2)$$

A widely used analog for continuous distributions is known as differential entropy:

$$H(Z) = -\int_Z p(z) \log p(z) dz. \quad (3)$$

Since our model estimates Gaussian densities, we can use the following expression to explicitly calculate differential entropy:

$$H(Z) = \frac{1}{2} \log\left\{(2\pi e)^n |\Sigma|\right\}. \quad (4)$$

In this case, the relationship between Σ and $H(Z)$ is obvious: the wider spread the learned Gaussian

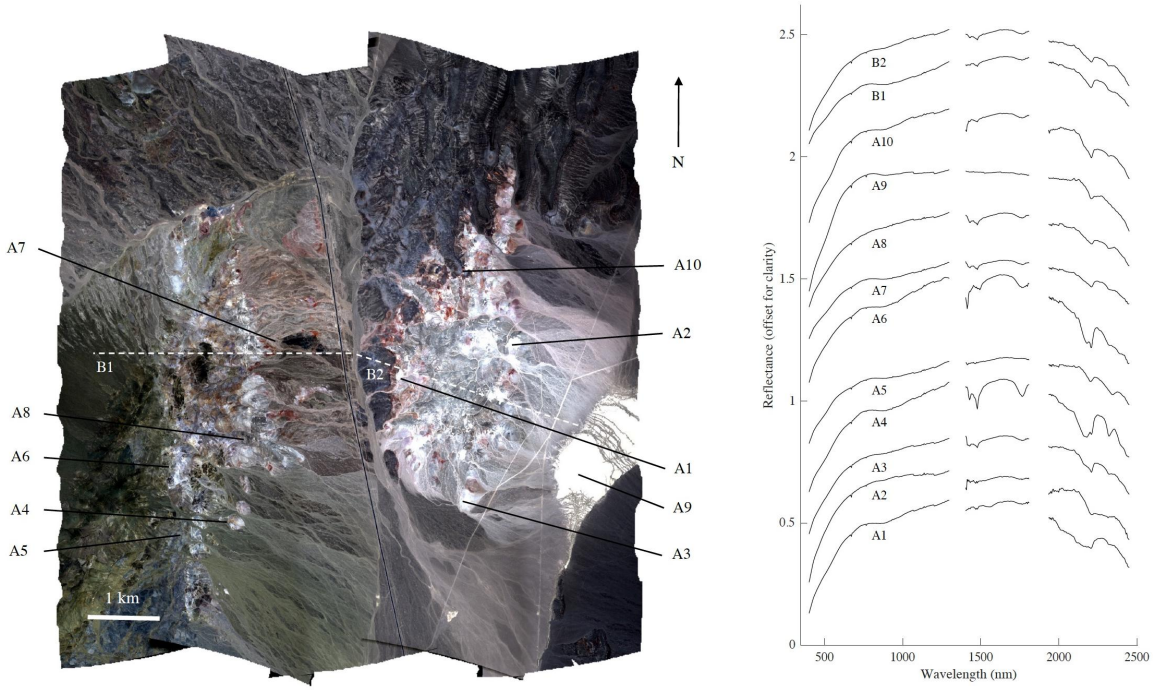

Figure 3: Left: Visible wavelength mosaic of Cuprite Hills, Nevada, as seen by the AVIRIS-NG sensor. Right: Representative reflectance spectra in the 0.4-2.5 μm range for points labeled on the mosaic image.

representation, the more uncertain the predictions. Using the simple yet powerful principle of maximum entropy sampling [21], one can efficiently learn about a system by collecting samples where prior information is less certain.

4 EXPERIMENT

We test our approach using spectroscopic measurements that are of high relevance for space exploration since they are used to determine the chemical composition and physical properties of objects [22]. We specifically work with reflectance spectroscopic observations of Cuprite, Nevada. It is a very well-studied region of high mineralogical diversity that is amenable to both remote sensing and *in situ* reflectance measurement in the 0.38-2.5 μm range [11].

We utilize a mosaic of NASA's Next Generation Airborne Visible Near Infrared Imaging Spectrometer (AVIRIS-NG) [24, 25] (Figure 3). We use a 50/50 split when producing the training and test sets, respectively.

The pixels of the AVIRIS-NG image cube are of high resolution (5 nm/channel, 3.7 m/pixel) and serve as the *in situ* spectra that would be obtained by a surface rover, specifically 97 channels in the 2.0-2.5 μm wavelength bands. To obtain remote sensing data again the AVIRIS-NG imaging spectrometer data was used, but modified to produce noisy, low-resolution images as proxy for orbital observation. Various synthetic responses are created by applying different levels of noise and resolution degradation to the Cuprite dataset. Specifically, two different levels of additive white Gaussian noise (AWGN) are used: low (SNR = 40 dB) and high (SNR = 30 dB). Five different levels of decimation are used: downsampling 97 channels to 10, 20, 30, 40, and 50, respectively.

The deep generative model was trained on a 2.9 GHz Intel Quad-Core i7 laptop without graphics processing unit (GPU). Training convergence is achieved after approximately 30 minutes.

Our deep generative model (DGM) is compared to two baseline methods. The first method (GMM) learns a Gaussian mixture model with 20 classes trained at full spectral resolution, and then conditioned on observed channels. The second method (INT) uses a Gaussian filter and cubic spline interpolation.

5 RESULTS

The first objective of this experiment is to evaluate and compare our method's ability to reconstruct *in situ* spectra from the aforementioned synthetic or-

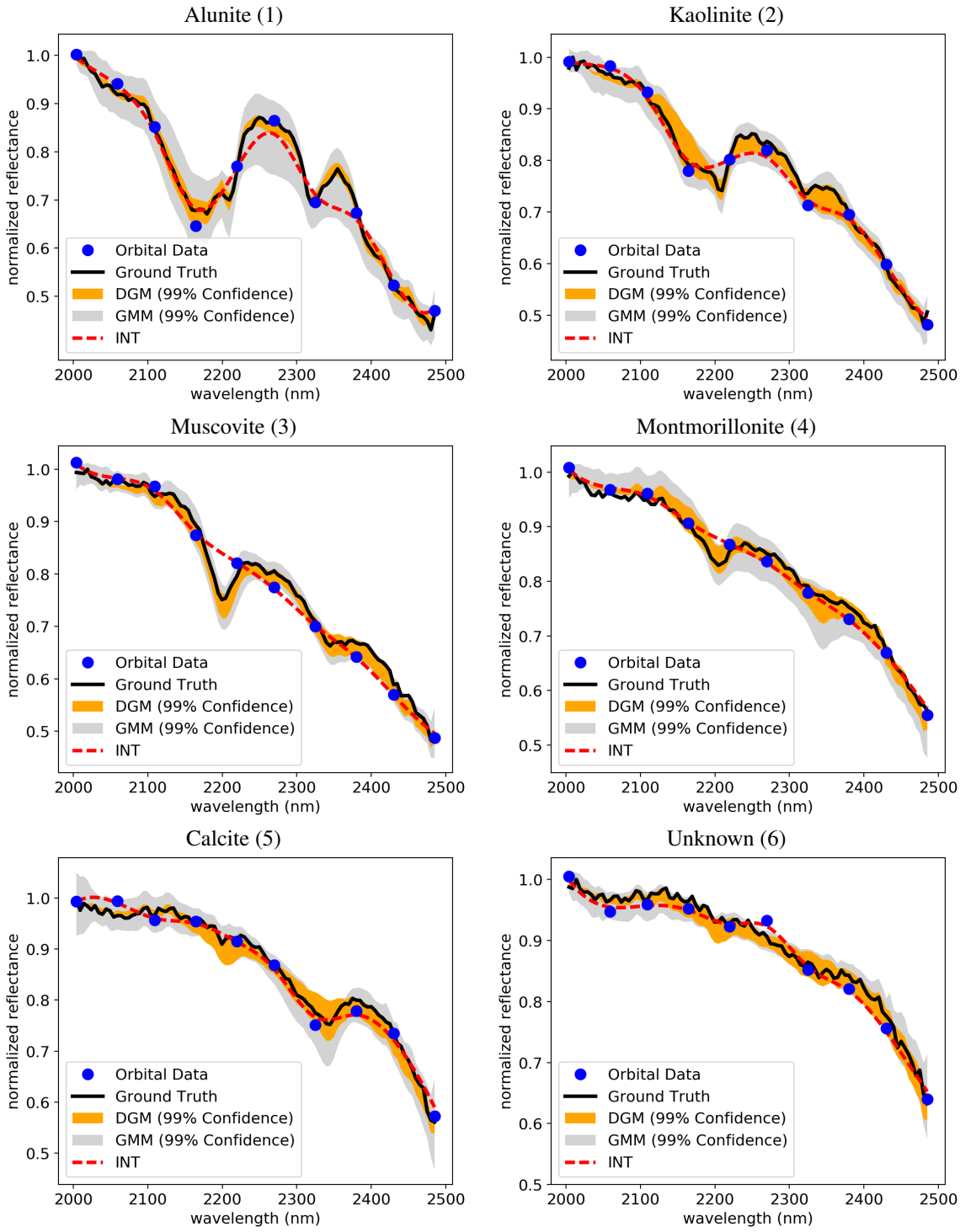

Figure 4: Example of in situ spectra predictions and ground truth values for six different minerals in Cuprite. Orbital measurements have 10 channels and a low noise level. The plots show in situ predictions generated by the interpolation (INT), Gaussian mixture model (GMM), and deep generative model (DGM) methods.

bital responses. The second objective is to identify effective sampling locations.

Figure 4 shows a qualitative visualization of *in situ* spectra predictions for the three methods us-

ing orbital data with 10 channels and low noise. Specifically, it contains spectra for five different minerals in Cuprite: alunite, kaolinite, muscovite, montmorillonite, and calcite; as well as for an unknown mineral. In spectral analysis, the most important features for chemical composition diagnosis are the absorption bands [22]. It can be observed that some of these features are preserved in the orbital data, whereas others tend to disappear. The DGM method is able to learn and infer these features, even when they may seem difficult to retrieve. GMM also does well at this, but its predictions are more broadly spread. Interpolation, INT, is the worst at capturing features and is also sensitive to noise (despite using a Gaussian filter).

We then evaluate the performance of the three methods with respect to the aforementioned levels of data degradation. Figure 5 shows the corresponding average mean squared errors. The DGM and GMM methods are evaluated using their maximum a posteriori estimates. All results are statistically significant using a 95% confidence. This figure reaffirms and formalizes many of the previous findings. DGM outperforms the baselines, especially when there is a large degradation in orbital measurements. The GMM baseline outperforms INT, but still has higher reconstruction errors than our method. DGM also seems to be much more robust since the errors are less sensitive to both noise and downsampling. As expected, the difference in performance between the three methods is reduced when orbital data has a high quality, since orbital measurements are more similar to *in situ* observations, i.e. there is less information loss.

Finally, an entropy or uncertainty map of the test set is shown in Figure 6, along with the locations of the spectra from Figure 4. This figure also shows a mineral map of Cuprite [11] generated by the Tetracorder algorithm, an expert system that has been widely used for automated mineral identification with imaging spectroscopy [26]. In here, black pixels indicate inconclusive classification results. It can be observed that high entropy regions match locations where the Tetracorder algorithm could not provide classifications. This suggests that our automatic experimental design approach is capable of identifying and displaying low certainty regions, which tend to be of special interest when mapping and characterizing an entire scene. In other words, the entropy map reveals locations that are especially difficult to map using

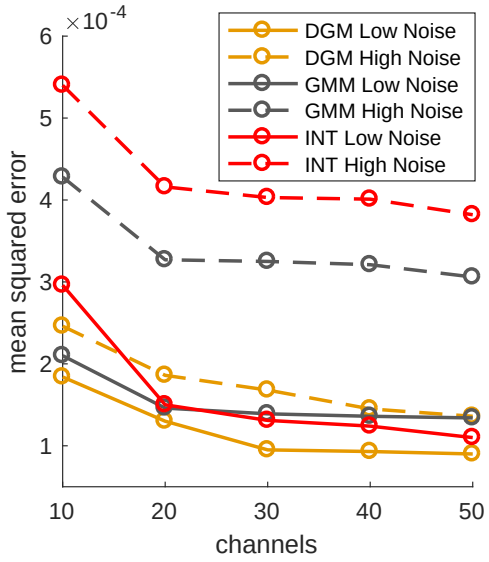

Figure 5: Average mean squared reconstruction errors of the three methods for various levels of noise and resolution degradation.

the contextual information from orbital data.

6 CONCLUSIONS

The study of remote planetary surfaces relies on the analysis of contextual orbital data, along with complementary *in situ* measurements. Since surface explorers face many operational challenges and constraints, it is important to identify locations that maximize information value.

We have proposed an approach that uses a deep generative model in order to learn a probabilistic representation connecting in situ and orbital data, and then estimates the information gain across the region to guide measurement planning. Our method is able to predict high resolution observations from low resolution orbital measurements with a higher accuracy than the baseline methods, and is also more robust to noise and resolution degradation. The learned probabilistic representations allow computation of the inherent entropy of the observations, revealing locations where contextual orbital data needs to be refined the most.

A great advantage of our formulation is that it learns underlying patterns without the need for labeled data, which are difficult to obtain when studying remote environments. Another encouraging aspect is that our model is efficiently trained on a laptop without using any GPUs, which is of critical importance when thinking of spacecraft or rover implementation.

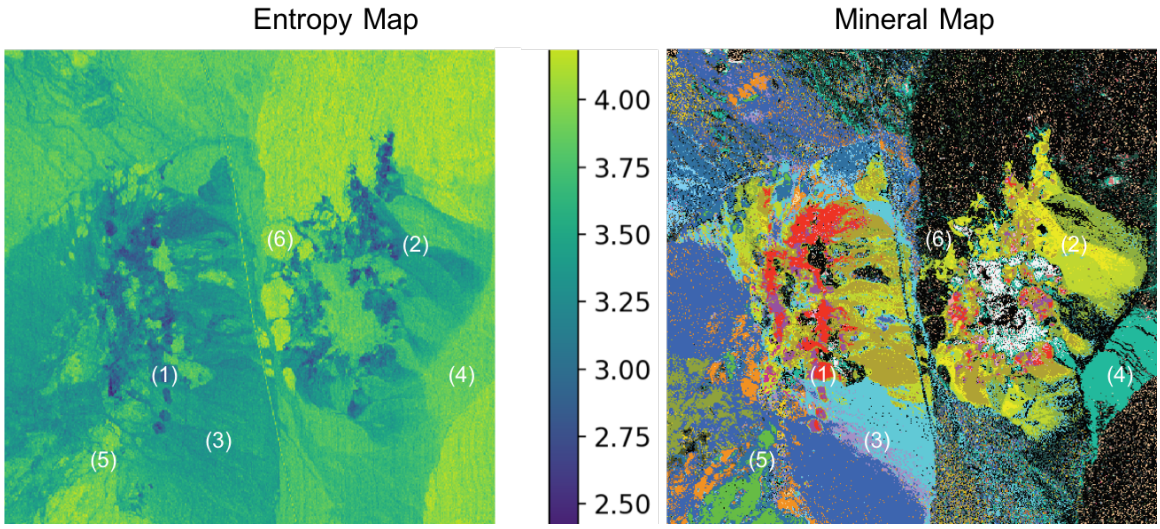

Figure 6: Left: Entropy map of Cuprite, and locations for the following minerals: alunite (1), kaolinite (2), muscovite (3), montmorillonite (4), calcite (5), and unknown (6). Right: Tetracorder mineral map [26], where black pixels indicate an inconclusive classification. These coincide with high-entropy regions.

Future investigations will apply this method to other sensors and domains besides spectroscopy, including multimodal data products. Finally, we are integrating this work with path planning algorithms that maximize science productivity given explicit exploration and traversability constraints.

Acknowledgements

This research was supported by the National Science Foundation National Robotics Initiative Grant #IIS-1526667. We acknowledge support of the NASA Earth Science Division for the use of AVIRIS-NG data. A portion of this research was performed at the Jet Propulsion Laboratory, California Institute of Technology, under a contract with the National Aeronautics and Space Administration.

References

[1] Zurek RW and Smrekar SE (2007) An overview of the Mars Reconnaissance Orbiter (MRO) science mission. In: *Journal of Geophysical Research: Planets*, 112(E5).

[2] Murchie S, Arvidson R, Bedini P et al. (2007) Compact Reconnaissance Imaging Spectrometer for Mars (CRISM) on Mars Reconnaissance Orbiter (MRO). In: *Journal of Geophysical Research: Planets*, 112(E5).

[3] Viviano-Beck CE et al. (2015) MRO CRISM Type Spectra Library. In: *NASA Planetary Data System*. Available at: `http://crismtypespectra.rsl.wustl.edu`.

[4] Clark RN, Swayze GA, Wise R et al. (2007) USGS Digital Spectral Library splib06a. In: *U.S. Geological Survey, Data Series 231*.

[5] Cover TM and Thomas JA (2006) *Elements of Information Theory*. Wiley-Interscience, Hoboken, New Jersey, 2nd edition.

[6] Pedersen L, Wagner M, Apostolopoulos D and Whittaker WR (2001) Autonomous robotic meteorite identification in Antarctica. In: *Proceedings 2001 ICRA. IEEE International Conference on Robotics and Automation*, volume 4, pp.4158–4165.

[7] Thompson DR, Smith T and Wettergreen D (2008) Information-Optimal Selective Data Return for Autonomous Rover Traverse Science and Survey. In: *IEEE Conference on Robotics and Automation*.

[8] Candela A, Thompson D, Dobrea EN and Wettergreen D (2017) Planetary robotic exploration driven by science hypotheses for geologic mapping. In: *2017 IEEE/RSJ International Conference on Intelligent Robots and Systems (IROS)*, pp.3811–3818.

[9] Gautam S, Roy BS, Candela A and Wettergreen D (2017) Science-aware exploration using entropy-based planning. In: *2017 IEEE/RSJ International Conference on Intelligent Robots and Systems (IROS)*, pp.3819–3825.

[10] Arora A, Fitch R and Sukkarieh S (2017) An approach to autonomous science by modeling geological knowledge in a Bayesian framework. In: *2017 IEEE/RSJ International Conference on Intel-*

ligent Robots and Systems (IROS), pp.3803–3810.
[11] Swayze GA, Clark RN, Goetz AF et al. (2014) Mapping advanced argillic alteration at Cuprite, Nevada, using imaging spectroscopy. In: *Economic Geology*, 109(5):pp.1179–1221.
[12] Hu Z, Yang Z, Salakhutdinov R and Xing EP (2018) On Unifying Deep Generative Models. In: *International Conference on Learning Representations*.
[13] Gómez-Bombarelli R, Wei JN, Duvenaud D et al. (2018) Automatic Chemical Design Using a Data-Driven Continuous Representation of Molecules. In: *ACS Central Science*, 4(2):pp.268–276.
[14] Regier J, Miller AC, McAuliffe J et al. (2015) Celeste: Variational inference for a generative model of astronomical images. In: *International Conference on Machine Learning*.
[15] Nasrollahi K and Moeslund TB (2014) Super-resolution: a comprehensive survey. In: *Machine Vision and Applications*, 25(6):pp.1423–1468.
[16] Dahl R, Norouzi M and Shlens J (2017) Pixel Recursive Super Resolution. In: *2017 IEEE International Conference on Computer Vision (ICCV)*, pp.5449–5458.
[17] Ledig C, Theis L, Huszár F, Caballero J et al. (2017) Photo-Realistic Single Image Super-Resolution Using a Generative Adversarial Network. In: *2017 IEEE Conference on Computer Vision and Pattern Recognition (CVPR)*. ISSN 1063-6919, pp.105–114.
[18] Goodfellow I, Pouget-Abadie J, Mirza M et al. (2014) *Generative adversarial nets*. In: Z Ghahramani, M Welling, C Cortes, ND Lawrence and KQ Weinberger (Editors), *Advances in Neural Information Processing Systems 27*, pp.2672–2680. Curran Associates, Inc.
[19] Kingma DP and Welling M (2013) Auto-encoding variational Bayes. In: *arXiv preprint arXiv:1312.6114*.
[20] Chaloner K and Verdinelli I (1995) Bayesian experimental design: a review. In: *Statistical Science*, 10(3):pp.273–304.
[21] Shewry MC and Wynn HP (1987) Maximum entropy sampling. In: *Journal of Applied Statistics*, 14(2):pp.165–170.
[22] Clark RN (1999) Spectroscopy of rocks and minerals, and principles of spectroscopy. In: *Manual of Remote Sensing*, 3:pp.3–58.
[23] Kingma DP and Ba J (2015) Adam: A Method for Stochastic Optimization. In: *Proceedings of the 3rd International Conference on Learning Representations (ICLR)*.
[24] Hamlin L, Green R, Mouroulis P et al. (2011) Imaging spectrometer science measurements for terrestrial ecology: AVIRIS and new developments. In: *Aerospace Conference, 2011 IEEE*, IEEE, pp.1–7.
[25] Thompson DR, Boardman JW, Eastwood ML et al. (2018) Imaging spectrometer stray spectral response: In-flight characterization, correction, and validation. In: *Remote Sensing of Environment*, 204:pp.850 – 860.
[26] Clark RN, Swayze GA, Livo KE et al. (2003) Imaging spectroscopy: Earth and planetary remote sensing with the USGS Tetracorder and expert systems. In: *Journal of Geophysical Research: Planets*, 108(E12). 5131.